J. Math. Biology 4, 149—169 (1977)

Journal of Mathematical Biology

Static Equilibrium Configurations of a Model Red Blood Cell

J. T. Jenkins, Ithaca, New York

Received June 9, 1976; accepted August 13, 1976

Summary

The membrane of the red blood cell is modeled as a fluid shell which resists bending and changes in area. The differential equations governing the mechanical equilibrium of such a membrane are derived and axisymmetric solutions are obtained numerically.

1. Introduction

The investigation of the mechanical basis for the shape of the red blood cell has engaged researchers for over a century. The normal mammalian red blood cells adopts a characteristic biconcave disc shape when at rest in the plasma. However as, for example, distilled water is added to the plasma the biconcave cell swells smoothly, becoming less biconcave, then an oblate ellipsoid and, finally, spherical. Careful observations by Canham and Parkinson (1970) indicate that the area of the red cell membrane remains constant during this swelling sequence; so, necessarily, the volume of material contained in the cell increases. If, once the spherical shape is attained, additional water is added to the plasma the cell eventually loses its hemoglobin and becomes an almost transparent "ghost". Both the ghost and the red cell can be made to traverse the swelling sequence in reverse, from the sphere to the biconcave disc, by reducing the amount of water relative to the plasma.

The interior of the red cell is generally regarded to be filled with a Newtonian fluid, while the red cell membrane is usually pictured as a double layer of long relatively rigid molecules with their hydrophillic heads buried in the aqueous solutions on either side of the membrane and their hydrophobic tails isolated in the interior of the bilayer. Other large molecules may penetrate the membrane or attach themselves to its interior or exterior.

There is no general agreement as to the mechanical properties of the red cell membrane. Most often it is considered to be a thin elastic, or viscoelastic, membrane which has as its preferred configuration the biconcave disc. For example, Zarda (1975) and Zarda et al. (1975), in a sequel to work by Fung (1966), Fung and Tong (1968) and Skalak et al. (1973), have proposed a model of this type and

introduced nonlinear elastic strain measures to describe deformations in the surface, a strain energy function which insures that changes in area are resisted more strongly than shear deformations, and a bending energy from a theory for thin elastic shells to obtain numerical solutions to the equations of equilibrium which give, as the pressure inside the cell is increased relative to that outside, shapes resembling the configurations adopted by the red cell swelling from the biconcave disc to the sphere. However, Canham (1970) has proposed that the bimolecular leaflet of the red cell membrane be viewed as a two dimensional incompressible fluid in which the long axes of the molecules of the bilayer orient normal to the surface of the membrane and prefer to remain parallel to each other. Shear deformations in the surface of the membrane are resisted only by viscous forces, local area changes are impossible, and bending deformations of a plane configuration are resisted by elastic couples arising from the induced misalignment of the long axes of the molecules. Singer and Nicolson (1972) have recently reviewed the evidence supporting the idea that the molecules of at least some biological membranes are mobile and that the membrane behaves as an oriented, two dimensional viscous fluid. Helfrich (1973) has discussed the physical foundations of a mechanical theory for lipid bilayers, the simplest such membrane, and has obtained mechanical equilibrium equations similar to those derived here, while Jenkins (1977) has placed mechanical theories of this type in the context of modern shell theory and has derived the general equations of mechanical equilibrium. Here we adopt this model and treat the red membrane as a liquid crystal surface which maintains local area and for which the bending energy is minimized in a plane configuration.

To assume that the molecule of the membrane prefer that the membrane be plane is not inconsistent with the existence of closed cells, for a plane membrane has edges on which either the hydrophobic tails of the molecules are exposed to water or extreme misalignment of molecules occur as the molecules orient to maintain their tails in the interior of the bilayer. As discussed by Fergason and Brown (1968), the competition between the surface energy of bending and the energy involved in maintaining an edge may, for large enough membranes, result in the membrane adopting a closed shape — eliminating the edge energy at the expense of some bending energy. The observations of, for example, Rand (1964, 1967) that the red cell when cut into two parts forms two closed surfaces support the idea that edges are energentically unfavorable and, in addition, seem to indicate that the red cell membrane is not an elastic envelope which has as its natural shape the biconcave disc.

As yet we have said nothing about any electrostatic effects which may influence the equilibrium of the membrane. As discussed by Lew (1970, 1971) and Adams (1972, 1973 a, 1973 b) for a membrane of constant area and thickness with uniform inner and outer surface change densities (supposed equal on any plane portion of the membrane), these effects are of two types: an induced polarization of the membrane due to the electric field across it and a modification of this electric field resulting from curvature of the membrane. Lew (1971) and Adams (1973 b) show that each of these effects are represented with reasonable accuracy by an energy density which is proportional to the square of the mean curvature of the membrane.

As will be seen, this is the form of the energy density utilized here, so these effects may be included by appropriately modifing the interpretation of the material coefficient.

In the context of this model of the membrane the biconcave disc is the shape adopted by a spherical cell when the sphere is buckled by an external excess of osmotic pressure over that internal. The swelling sequence is generated by reducing this osmotic pressure excess while allowing material to pass through the membrane. In what follows the equations of mechanical equilibrium for the membrane are derived from a principle of virtual work.

These equations are then specialized in order to study axisymmetric deformations of a sphere subjected to a uniform external hydrostatic pressure. The system of nonlinear, ordinary differential equations governing the axisymmetric deformations are solved numerically and one family of solutions, evolving as the external osmotic pressure is increased from the first possible bifurcation predicted by the linearized theory, is shown to give shapes resembling the swelling sequence. The total energy of these solutions is less than that of the sphere, which is always a solution. There is, however, a second family of solutions, also evolving from the first bifurcation, which exists over the range of pressures of the swelling sequence and which involve even less total energy. The configurations of this second family are, apparently, not observed.

2. The Equations of Mechanical Equilibrium

The differential geometry which we require is given in greater detail in the book by Eisenhart (1974).

The membrane is represented as a closed surface A in space, the position vector $\underline{r}$ to a point on A being given in terms of two parameters u^α (Greek indices takes the values 1 and 2) which label material points

$$\underline{r} = \underline{r}(u^\alpha). \tag{2.1}$$

The vectors

$$\underline{a}_\alpha \equiv \underline{r}_{,\alpha} \tag{2.2}$$

(where a comma indicates a partial derivative) are tangent to the u^α curves. The first fundamental form $a_{\alpha\beta}$ of A,

$$a_{\alpha\beta} \equiv \underline{a}_\alpha \cdot \underline{a}_\beta = a_{\beta\alpha}, \tag{2.3}$$

possesses a unique inverse $a^{\alpha\beta}$ provided that

$$a \equiv \det a_{\alpha\beta} \neq 0. \tag{2.4}$$

In which case reciprocal vectors $\underline{a}^\alpha$ are defined by:

$$\underline{a}^\alpha = a^{\alpha\beta}\, \underline{a}_\beta \tag{2.5}$$

(with repeated indices summed). The unit normal $\underline{n}$ to A is given by

$$\sqrt{a}\, \underline{n} = \underline{a}_1 \times \underline{a}_2. \tag{2.6}$$

Because $\underline{n} \cdot \underline{n} = 1$,

$$\underline{n}_{,\alpha} = -b_{\alpha\beta}\,\underline{a}^{\beta}; \tag{2.7}$$

$b_{\alpha\beta}$ is called the second fundamental form of A,

$$b_{\alpha\beta} = -\underline{n}_{,\alpha} \cdot \underline{a}_{\beta} = \underline{n} \cdot \underline{a}_{\alpha,\beta} = b_{\beta\alpha}. \tag{2.8}$$

Alternatively,

$$\underline{a}_{\alpha|\beta} = b_{\alpha\beta}\,\underline{n}, \tag{2.9}$$

where the stroke denotes covariant differentiation based on $\alpha_{\alpha\beta}$. The mean curvature h and the total curvature k of A are defined in terms of $b_{\alpha\beta}$ by

$$h = \tfrac{1}{2}\, b^{\beta}_{\beta},\quad k = \det b^{\alpha}_{\beta}. \tag{2.10}$$

If the membrane is modeled as a two dimensional incompressible fluid with the long axes of the molecules normal to the surface and the intermolecular forces promoting parallel orientation, the free energy w per unit area of A should depend upon the local deviation of the molecular orientation from parallel. As discussed by Jenkins (1976), the only free energy function which is compatible with the fluidity of the surface and is unaffected by rigid rotations depends at most upon h and k, each of which contain the derivatives $\underline{n}_{,\alpha}$ in combination with the reciprocal vectors $\underline{a}^{\beta}$. If, in addition, the inside and the outside of the membrane are indistinguishable

$$w = w\,(h^2, k), \tag{2.11}$$

the simplest form being

$$w = c\,h^2 + c_1\,k \tag{2.12}$$

where c and c_1 are constants. In his study of lipid bilayers Helferich (1973) assumes that the interior and the exterior of the membrane are distinguishable and includes a term linear in h in order to treat membranes with a natural, or spontaneous, curvature. As we pointed out in the introduction, it is not necessary to include this term to explain the existence of closed membranes. If we restrict attention to closed surfaces which may be smoothly deformed into, say, a sphere, then by Gauss's theorem the contribution of the last term to the total free energy W

$$W = \int_{A} w\,dA \tag{2.13}$$

is the same for all such surfaces.

To obtain the equations of mechanical equilibrium of the red cell membrane we introduce a one parameter family of comparison surfaces

$$\underline{r} = \underline{r}\,(u^{\alpha}, \varepsilon) \tag{2.14}$$

and equate the variation δW to the working of the applied forces in the variation $\delta \underline{r}$, where

$$\delta W \equiv \frac{\partial W(\varepsilon)}{\partial \varepsilon}\bigg|_{\varepsilon=0},\quad \delta \underline{r} \equiv \frac{\partial \underline{r}\,(u^{\alpha}, \varepsilon)}{\partial \varepsilon}\bigg|_{\varepsilon=0}. \tag{2.15}$$

As mentioned above, the term involving k contributes nothing, so we write

$$\delta \int_A c h^2 \, dA = -\bar{p} \int_A \underline{n} \cdot \delta \underline{r} \, dA \tag{2.16}$$

where $\bar{p}$ is the excess of the pressure exterior over that interior and is assumed constant. Incompressibility requires that the local area element does not vary so, with $dA = \sqrt{a}\, du^1 du^2$,

$$\delta \sqrt{a} = 0. \tag{2.17}$$

Introducing the Lagrange multiplier $\gamma(u^\alpha)$ associated with this constraint, the variation in the energy may be written as

$$\delta W = \int_A (2 c h \delta h - \gamma \delta \sqrt{a}) \, dA. \tag{2.18}$$

Here again our approach differs from that of Helferich (1973) who uses a global area constraint and introduces a constant Lagrange multiplier.

A calculation gives

$$\delta \sqrt{a} = \sqrt{a}\, \underline{a}^\alpha \cdot \delta \underline{a}_\alpha \tag{2.19}$$

$$\delta h = \tfrac{1}{2} a^{\alpha\beta} \underline{n}_{,\alpha} \cdot \delta \underline{a}_\beta - \tfrac{1}{2} \underline{a}^\alpha \cdot \delta \underline{n}_{,\alpha} \tag{2.20}$$

and

$$\delta \underline{n} = -\underline{a}^\beta (\underline{n} \cdot \delta \underline{a}_\beta); \tag{2.21}$$

so

$$\delta W = \int_A [(-\gamma \sqrt{a}\, \underline{a}^\beta + c h \, \underline{n}_{,\alpha} a^{\alpha\beta}) \cdot \delta \underline{a}_\beta - c h \, \underline{a}^\alpha \cdot \delta \underline{n}_{,\alpha}] \, dA. \tag{2.22}$$

Integrating by parts the last term, and utilizing the surface divergence theorem and equation (2.21), we obtain

$$-\int_A c h \, \underline{a}^\alpha \cdot \delta \underline{n}_{,\alpha} \, dA = -\int_A (c h \, \underline{a}^\alpha)_{|\alpha} \cdot \underline{a}^\beta (\underline{n} \cdot \delta \underline{a}_\beta) \, dA \tag{2.23}$$

$$= -\int_A c h_{,\alpha} a^{\alpha\beta} \underline{n} \cdot \delta \underline{a}_\beta \, dA. \tag{2.24}$$

A second integration by parts and application of the divergence theorem yields

$$\delta W = \int_A [(\gamma \sqrt{a}\, a^{\alpha\beta} + c h \, b^{\alpha\beta}) \underline{a}_\beta + c h_{,\beta} a^{\alpha\beta} \underline{n}]_{|\alpha} \cdot \delta \underline{r} \, dA. \tag{2.25}$$

With this, the principle of virtual works becomes

$$\int_A \{[(\gamma \sqrt{a}\, a^{\alpha\beta} + c h \, b^{\alpha\beta}) \underline{a}_\beta + c h_{,\beta} a^{\alpha\beta} \underline{n}]_{|\alpha} + \bar{p} \, \underline{n}\} \cdot \delta \underline{r} \, dA; \tag{2.26}$$

Hence

$$[(\gamma \sqrt{a}\, a^{\alpha\beta} + c h \, b^{\alpha\beta}) \underline{a}_\beta + c h_{,\beta} a^{\alpha\beta} \underline{n}]_{|\alpha} = -\bar{p} \, \underline{n}. \tag{2.27}$$

The normal component of this equilibrium equation is

$$2\gamma \sqrt{a}\, h + c h \, b^{\alpha\beta} b_{\alpha\beta} + c (h_{,\beta} a^{\alpha\beta})_{|\alpha} = -\bar{p}, \tag{2.28}$$

while the tangential components are

$$(\gamma \sqrt{a}\, \delta^\alpha_\beta + c h \, b^\alpha_\beta)_{|\alpha} - c h_{,\alpha} b^\alpha_\beta = 0. \tag{2.29}$$

In the Appendix the correspondence between these equilibrium equations and the equations of classical thin shell theory is indicated. Now the second fundamental form satisfies the Mainardi-Codazzi equations

$$b_{\alpha\beta\,|\,\gamma}=b_{\alpha\gamma\,|\,\beta}; \tag{2.30}$$

so

$$b^{\alpha}_{\beta\,|\,\alpha}=b^{\alpha}_{\alpha,\,\beta}=2\,h_{,\beta}. \tag{2.31}$$

With this, the tangential equilibrium equations become

$$(\gamma\sqrt{a}+c\,h^2)_{,\beta}=0, \tag{2.32}$$

or

$$\gamma\sqrt{a}+c\,h^2=\bar{d} \tag{2.33}$$

where $\bar{d}$ is a constant. This equation determines the Lagrange multiplier γ. With this and the appropriate specialization of the identity

$$b^{\alpha\beta}\,b_{\beta\gamma}=2\,h\,b^{\alpha}_{\gamma}-k\,\delta^{\alpha}_{\gamma}, \tag{2.34}$$

the normal component of the equilibrium equation is

$$\frac{c}{\sqrt{a}}(\sqrt{a}\,a^{\alpha\beta}\,h_{,\beta})_{,\alpha}+2\,h\,[\bar{d}+c\,(h^2-k)]=-\bar{p}, \tag{2.35}$$

where the divergence has been expressed in terms of partial derivatives.

3. Axisymmetric Deformations of a Sphere

We seek equilibrium configurations which are axisymmetric deformations of a sphere. All quantities bearing the dimension of length are nondimensionalized by the radius ρ of the sphere and we confine our attention to a sphere of

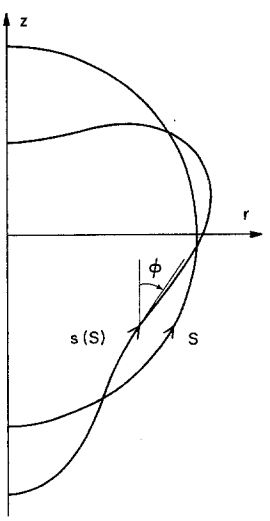

Fig. 1. The coordinates, arc lengths and tangent angle

unit radius. The material parameters are the azimuthal angle θ and the arc length S from the axis of symmetry to a point on the sphere (Fig. 1). The arc length to the corresponding point on the deformed surface is $s=s(S)$ and the angle between the tangent to a line $\theta=$constant and the axis of symmetry is $\phi=\hat{\phi}(s)=\phi(S)$. If r and z are considered to be functions of s, then the unit tangent has r and z components

$$r'=\sin\hat{\phi},\quad z'=\cos\hat{\phi}, \tag{3.1}$$

respectively, where the prime denotes a derivative with respect to s.

The nonvanishing components of the first fundamental form are

$$a_{\theta\theta}=r^2 \quad \text{and} \quad a_{SS}=(\dot{s})^2, \tag{3.2}$$

where a dot indicates a derivative with respect to S. Then

$$\sqrt{a}=r\dot{s}, \tag{3.3}$$

and, upon evaluating this for the sphere, the incompressibility condition becomes

$$r\dot{s}=R, \tag{3.4}$$

where a capital letter labels a quantity associated with the sphere.

The nonvanishing components of the second fundamental form are

$$b_{\theta\theta}=-r\cos\phi \quad \text{and} \quad b_{SS}=\frac{R}{r}\dot{\phi}; \tag{3.5}$$

so

$$h=\frac{1}{2}\left(\frac{r}{R}\dot{\phi}-\frac{\cos\phi}{r}\right) \quad \text{and} \quad k=-\dot{\phi}\frac{\cos\phi}{R}. \tag{3.6}$$

For the sphere $\Phi=\frac{\pi}{2}-S$ and the expressions for the components of the unit tangent integrate to

$$R=\sin S \quad \text{and} \quad Z=-\cos S, \tag{3.7}$$

while

$$H=-1 \quad \text{and} \quad K=+1. \tag{3.8}$$

We introduce the non-dimensional pressure p,

$$p=\rho^3 c^{-1}\bar{p}, \tag{3.9}$$

set

$$d=\rho^3 c^{-1}\bar{d}, \tag{3.10}$$

and nondimensionalize the transverse shear of the Appendix,

$$q\equiv\rho^2 c^{-1} Q^S. \tag{3.11}$$

Then the nondimensional equilibrium equation and the subsidiary equations for r and z may be written as the systems of five first order equations

$$\dot{q}=-\cot S\, q-2h\left[d+h^2+\frac{\cos\phi}{r}\left(2h+\frac{\cos\phi}{r}\right)\right]-p, \tag{3.12}$$

$$\dot{h}=\frac{\sin^2 S}{r^2}\,q, \tag{3.13}$$

$$\dot{\phi}=\frac{2\sin S}{r}\,h+\frac{\sin S}{r^2}\cos\phi, \tag{3.14}$$

$$\dot{r}=\frac{\sin S}{r}\sin\phi, \tag{3.15}$$

and

$$\dot{z}=\frac{\sin S}{r}\cos\phi, \tag{3.16}$$

for $0\leq S\leq\pi$. The physical boundary conditions appropriate to the axisymmetric configuration are vanishing transverse shear on the axis and continuity of the tangent on the axis:

$$q(0)=q(\pi)=0,\ \phi(0)=\tfrac{\pi}{2},\ \phi(\pi)=-\tfrac{\pi}{2},\ r(0)=0,\ z(\tfrac{\pi}{2})=0, \tag{3.17}$$

the last condition fixing the location of the configuration.

If equation (3.12) is multiplied by $\sin S\sin\phi$ and integrated from 0 to π, the use of equation (3.14) and the boundary conditions (3.17) yield $r(\pi)=0$; so this condition is satisfied for any solution. Solutions of (3.12)—(3.16) in the interval $0\leq S\leq\frac{\pi}{2}$ which satisfy the boundary conditions

$$q(0)=q(\tfrac{\pi}{2})=0,\ \phi(0)=\tfrac{\pi}{2},\ \phi(\tfrac{\pi}{2})=0,\ r(0)=0,\ z(\tfrac{\pi}{2})=0, \tag{3.18}$$

we call symmetric solutions, for the resulting configuration has the plane of symmetry $z=0$. Axisymmetric configurations without a plane of symmetry are called asymmetric solutions.

The sphere is always a solution of the differential equations (3.12)—(3.16) and the boundary conditions (3.17), provided that the constant d takes the value $p/2$. In order to determine at what values of the pressure other solutions are possible in the neighborhood of the sphere, we linearize the differential equations and boundary conditions about the sphere and obtain

$$\frac{1}{\sin S}(\sin S\,\dot{h}_1)^{\cdot}+p\,h_1=2\,d_1, \tag{3.19}$$

$$(\sin S\,\phi_1)^{\cdot}=2\sin S\,h_1, \tag{3.20}$$

$$(\sin S\,r_1)^{\cdot}=\sin^2 S\,\phi_1, \tag{3.21}$$

$$\dot{z}_1=r_1-\cos S\,\phi_1; \tag{3.22}$$

where the subscript labels small perturbations from the values of the quantities associated with the sphere. Equation (3.19) is, essentially, the linearized equation obtained by Helfrich (1973). The boundary conditions are

$$\dot{h}_1(0)=\dot{h}_1(\pi)=\phi_1(0)=\phi_1(\pi)=r_1(0)=z_1(\tfrac{\pi}{2})=0. \tag{3.23}$$

The particular solution of (3.19) leads to a solution of (3.20) which is not compatible with the end conditions; consequently $d_1=0$, and the modification to the constant

d is of higher order. Then, when

$$p=l(l+1), \quad l=1, 2, 3 \ldots, \tag{3.24}$$

solutions of equation (3.19) are

$$h_1=\varepsilon P_l(\cos S), \tag{3.25}$$

where $P_l(\cos S)$ are the Legendre polynomials and the small but otherwise arbitrary constant ε may be positive or negative; however when l is unity the corresponding solution of (3.20) can not satisfy both end conditions, so this polynomial must be excluded. At the remaining values of the pressure given by (3.24) solutions other than the sphere are possible. When l is even the solutions are symmetric; when l is odd, the solutions are asymmetric. For symmetric solutions different choices of the sign of ε yield distinct configurations; asymmetric solutions corresponding to different signs are related by a rotation. Thus the linear theory indicates that there are no solutions in the neighborhood of the sphere for values of p less than 6. For $p=6$ the first bifurcation occurs and two distinct symmetric solutions, different from the sphere, are possible. For values of p greater than 6 but less than 12 no solutions exist near the sphere. At $p=12$ a second bifurcation takes place and a single distinct asymmetric solution is first obtained from the sphere. Other bifurcations follow the same pattern; here we shall concentrate on the solutions to the nonlinear equations which evolve from the first two bifurcations.

In order to determine whether nonspherical solutions to the nonlinear equations are likely to be observed, we compare the total energy of a deformed configuration to that of the sphere. The excess of the total nondimensional energy ΔE of the deformed state over that of the sphere is the difference of their total free energies less the working of the pressure in the deformation of the sphere:

$$\Delta E=2\pi \int_0^{\pi} \left[(h^2-1)+\frac{p}{3}(r\cos\phi-z\sin\phi-1)\right] \sin S\, dS, \tag{3.26}$$

where we have used the formula

$$\int_v dv=\frac{2\pi}{3}\int_0^{\pi} r(r\dot{z}-z\dot{r})\, dS \tag{3.27}$$

in calculating the volume change in a deformation of the sphere. When ΔE is negative the deformed configuration involves less total energy than the sphere. The product of ΔE and c is the energy difference bearing the appropriate units.

4. Numerical Results

Numerical solutions of the nonlinear differential equations (3.12)—(3.15) were obtained using the quasilinearization method discussed by Bellman and Kabala (1965). The six dimensional vector y with components

$$y_i=(q, h, \phi, r, z, d) \tag{4.1}$$

is to satisfy the differential equation

$$\dot{\underset{\sim}{y}} = \underset{\sim}{f}(\underset{\sim}{y}, S; p), \tag{4.2}$$

where

$$f_1 = -y_1 \cos S - 2 y_2 [y_6 + y_2^2 + y_4^{-1} \cos y_3 (2 y_2 + y_4^{-1} \cos y_3)] - p, \tag{4.3}$$

$$f_2 = y_4^{-2} y_1 \sin^2 S, \tag{4.4}$$

$$f_3 = y_4^{-1} (2 y_2 + y_4^{-1} \cos y_3) \sin S, \tag{4.5}$$

$$f_4 = y_4^{-1} \cos y_3 \sin S, \tag{4.6}$$

$$f_5 = y_4^{-1} \sin y_3 \sin S, \tag{4.7}$$

and

$$f_6 = 0. \tag{4.8}$$

For a symmetric solution we restrict attention to the interval $0 \leq S \leq \frac{\pi}{2}$ and employ the boundary conditions

$$y_1(0) = y_1(\tfrac{\pi}{2}) = y_3(\tfrac{\pi}{2}) = y_4(0) = y_5(\tfrac{\pi}{2}) = 0,\ y_3(0) = \tfrac{\pi}{2}. \tag{4.9}$$

Given p, an initial guess $\underset{\sim}{y}^{(0)}(S)$ is made and used to initiate an internation scheme in which the linear differential equation governing the n-th iteration is

$$\dot{\underset{\sim}{y}}^{(n)} = \underset{\approx}{\nabla f}\, \underset{\sim}{y}^{(n)} - \underset{\sim}{F}, \tag{4.10}$$

where the components of the matrix $\underset{\approx}{\nabla f}$ are the partial derivatives of f_i with respect to y_k, $f_{i,k}$, evaluated at $y^{(n-1)}$ and

$$\underset{\sim}{F} = \underset{\sim}{F}(\underset{\sim}{y}^{(n-1)}, S; p) \equiv -\underset{\approx}{\nabla f}\, \underset{\sim}{y}^{(n-1)} + \underset{\sim}{f}(\underset{\sim}{y}^{(n-1)}, S; p). \tag{4.11}$$

For each n, numerical solutions to four initial value problems are obtained. The first, $\underset{\sim}{y}_I^{(n)}$, is the solution to the inhomogeneous differential equation and the initial conditions $(y_I^{(n)})_i = (0, 0, \frac{\pi}{2}, 0, 0, 0)$. The remaining three, $\underset{\sim}{y}_{II}^{(n)}$, $\underset{\sim}{y}_{III}^{(n)}$, $\underset{\sim}{y}_{IV}^{(n)}$, satisfy the homogeneous differential equation, obtained by setting $\underset{\sim}{F} = 0$, and the initial conditions $(y_{II}^{(n)})_i = (0, 1, 0, 0, 0, 0)$, $(y_{III}^{(n)})_i = (0, 0, 0, 0, 1, 0)$ and $(y_{IV}^{(n)})_i = (0, 0, 0, 0, 0, 1)$ respectively. A linear combination of these solutions is formed

$$\underset{\sim}{y}^{(n)} = \underset{\sim}{y}_I^{(n)} + C_{II}\, \underset{\sim}{y}_{II}^{(n)} + C_{III}\, \underset{\sim}{y}_{III}^{(n)} + C_{IV}\, \underset{\sim}{y}_{IV}^{(n)}, \tag{4.12}$$

and the constants C_{II}, C_{III}, C_{IV} are determined by the boundary conditions at $S = \frac{\pi}{2}$:

$$y_1^{(n)}(\tfrac{\pi}{2}) = y_3^{(n)}(\tfrac{\pi}{2}) = y_5^{(n)}(\tfrac{\pi}{2}) = 0. \tag{4.13}$$

This solution to the linear equation is then used as the basis for the next iteration and the iterations are carried out until the difference between two successive iterations is made as small as one desires. The computation of the asymmetric solution is done in essentially the same way, integrating foreward from $S = 0$ to $\frac{\pi}{2}$ and backward from $S = \pi$ to $\frac{\pi}{2}$ and employing continuity conditions at $\frac{\pi}{2}$. Because of the singularity of the differential equation on the axis of symmetry, care must be taken when starting the solutions on the axis.

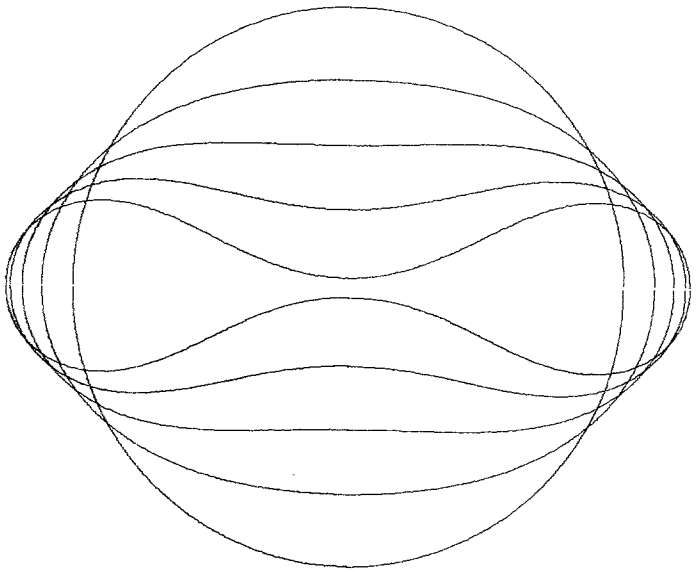

Fig. 2. Cross section from the family 6^+. $p = 6.0$, 6.5, 7.0, 7.5, 8.0. The deformation increases with pressure. The axis of symmetry is vertical

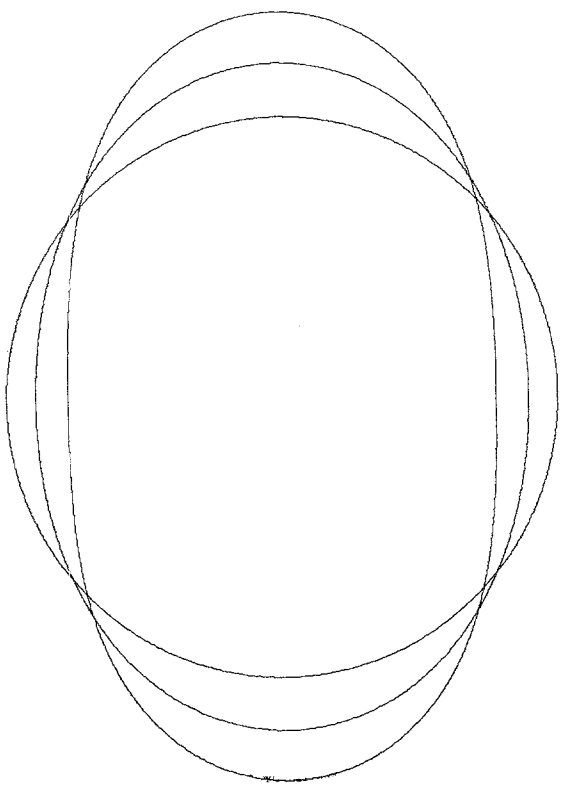

Fig. 3a. Cross section from the first branch of the family 6^-. $p = 6.00$, 5.80, 5.64. The deformation increases as the pressure decreases

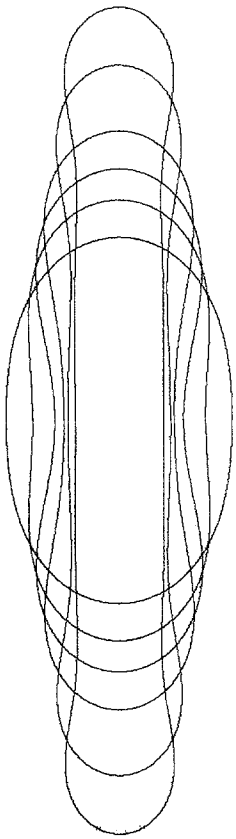

Fig. 3 b. Cross sections from the second branch of the family 6^-. $p = 5.64, 8, 12, 20, 30, 40$. The deformation increases with pressure

In Fig. 2 is drawn a succession of configurations obtained using this scheme of computation for the family of symmetric solutions, called 6^+, bifurcating from $p=6$ with $\varepsilon>0$. For this family the deformation of the sphere increases as the pressure is increased in the range of pressure shown. The resemblance of these cross sections to those exhibited by the red cell while swelling is striking. The cross section closest to the biconcave shape of the normal red cell is evidently attained at a value of p between 7.5 and 8.0. For values of p above 8.03 the upper and lower surfaces of the configurations intersect and the solutions beyond this point are of no physical interest.

In Fig. 3 a are drawn cross sections of two members of the family 6^- bifurcating from $p=6$ with $\varepsilon<0$. Here increasing deformation is obtained by lowering p from 6.00 to 5.64. At $p=5.64$ a second branch of solutions of the family 6^- emerges. On this branch the deformation proceeds as the pressure is increased over the relatively large range of Fig. 3 b.

The behavior of the asymmetric family bifurcating from $p=12$ is similar to that of 6^-. From $p=12$ to $p=10.39$ the deformation of the sphere increases as the pressure is lowered (Fig. 4 a). At $p=10.39$ begins a second branch on which the deformation continues as the pressure is raised (Fig. 4 b).

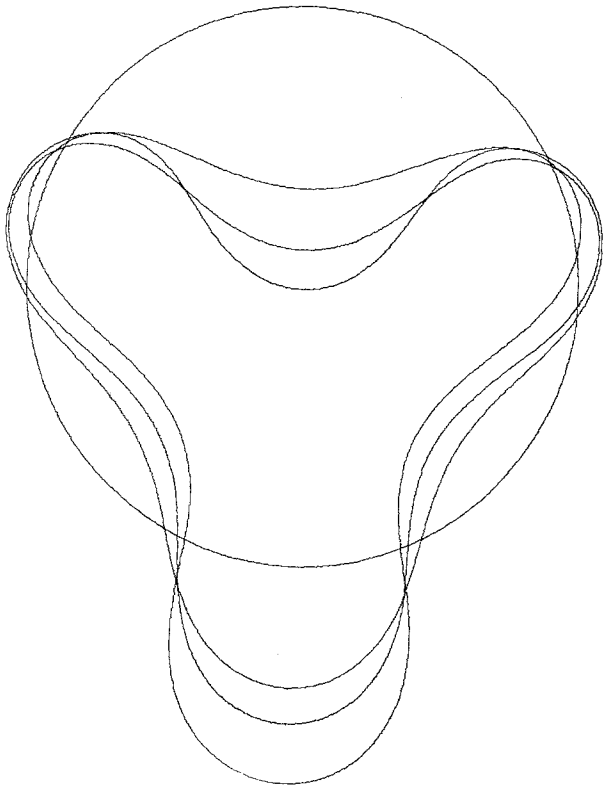

Fig. 4a. Asymmetric cross sections on the first branch of the family bifurcating from $p = 12$. $p = 12$, 11.50, 11.00, 11.39. The deformation increases as the pressure decreases

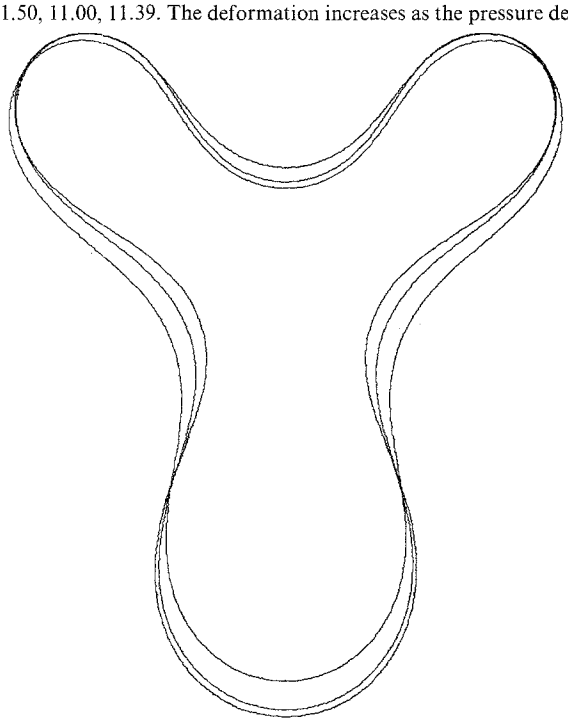

Fig. 4b. Asymmetric cross sections on the second branch of the family bifurcating from $p = 12$. $p = 10.39$, 11.00, 12.00. The deformation increases with pressure

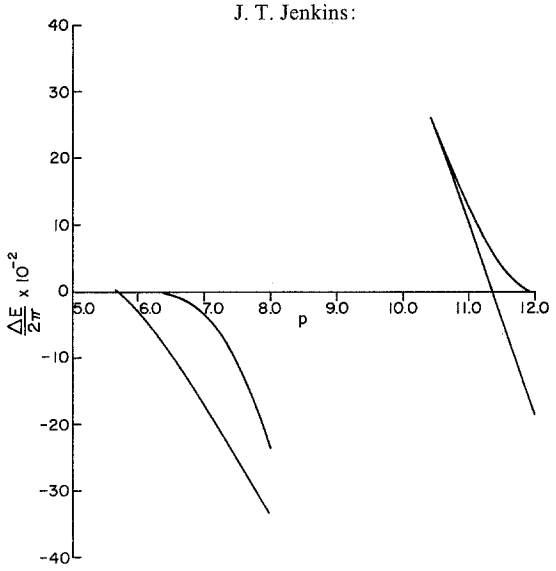

Fig. 5a. The energy difference versus the pressure

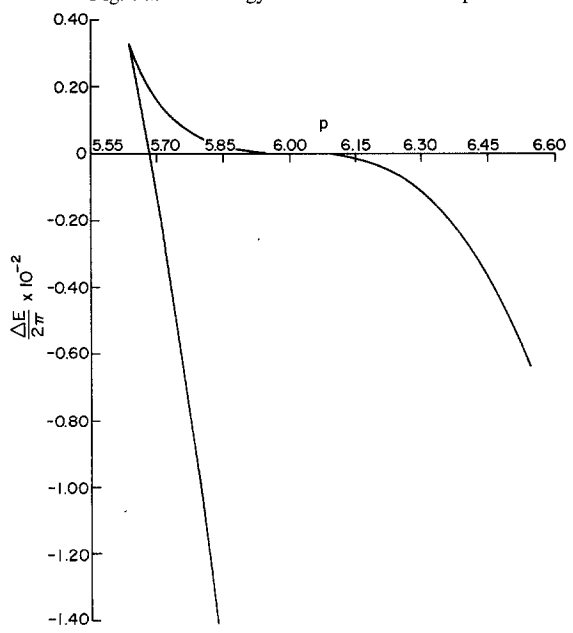

Fig. 5b. The energy difference versus the pressure in the neighborhood of $p = 6.00$

The relationship between the various solution branches and the pressure is made clear in Fig. 5a in which p is plotted versus one measure of the amplitude of the deformation, ΔE. In Fig. 5b the pressure-energy graph for the families 6^+ and 6^- is shown in greater detail in the neighborhood of the bifurcation. Note that the family 6^+ always involves less total energy than that of the sphere. The energetics of the family 6^- are more complicated. For every value of p between 5.64 and 6.00 there exist two members of 6^-; for $5.64 \leq p < 5.69$ both solutions require more energy than the sphere, for $p > 5.69$ one solution involves more energy than the sphere, the other less. In the range of pressure over which the families 6^+ and 6^-

both exist, the member of the family 6^- always involves less energy than the corresponding member of the family 6^+. The relationship between p and ΔE for the asymmetric branch is similar to, but more dramatic than, that for the family 6^-

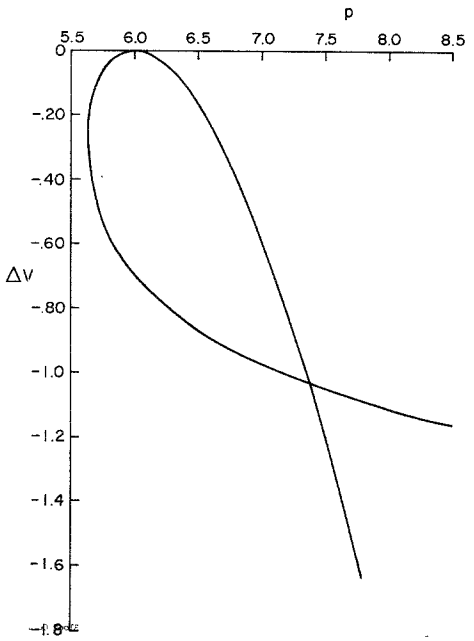

Fig. 6. The volume difference versus the pressure for the symmetric solutions

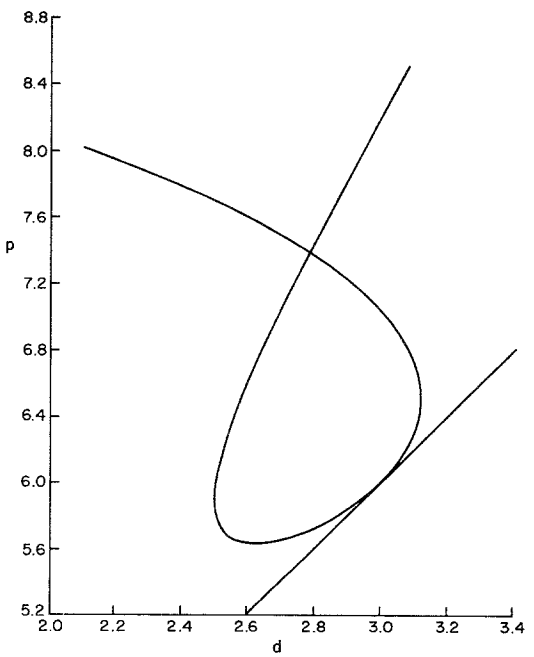

Fig. 7. The pressure versus the negative of the mean membrane stress for the symmetric solutions and the sphere

Because solutions of both families 6^+ and 6^- exist over the range of pressure $6.00 \leq p \leq 8.03$ we wish to include as much information about these families as can be presented compactly. The relationship between the pressure and the change in volume from the sphere is given for these families in Fig. 6. In Fig. 7 we plot the surface pressure d (see equation (A.15) of the Appendix) versus p for both families and for the sphere. It is remarkable that at $p=7.4$ both the volume and the mean surface pressure of the two solutions are equal. The cross sections of these two shapes are shown superposed in Fig. 8.

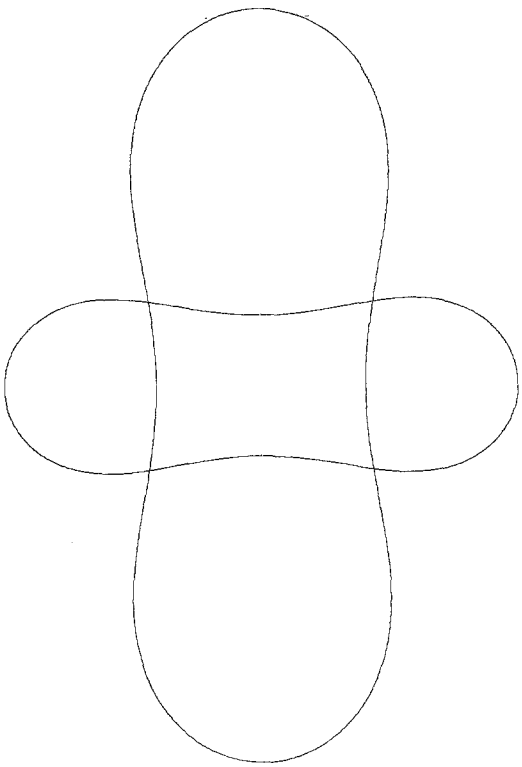

Fig. 8. The cross sections from the families 6^- and 6^+ at $p = 7.4$

The numerical solutions which we have presented above were selected from those which we have obtained either because they were of biological interest or because they illustrated important features of the nonlinear theory. The asymmetric solutions were included for the latter reason although they were generated in an unsuccessful effort to obtain as solutions the cup shaped red cells observed by Canham (1970) and Canham and Parkinson (1970). To satisfy our curiousity, we have obtained solutions in the three families discussed above outside of the range of pressures indicated in the figures and we have investigated the two symmetric families bifurcating from $p=20$. None of these solutions appears to be of biological interest.

5. Conclusion

To have obtained the shape of the biconcave disc and the configurations of the swelling sequence as solutions to the equilibrium equations derived for the liquid crystal model of the membrane is encouraging. However the existence of the second family of solutions over the same range of pressures, involving less total energy and, at least in terms of volume, close to the first family may be, in light of fact that these configurations seem not to be observed, puzzling.

If we assume for the moment that the membrane model is correct, the fact that these shapes are not seen is an indication that the comparison of the total energy of two solutions is not a good indication of which solution will be realized. First, we have not determined whether or not any of the numerical solutions corresponds to a local minimum of the total energy. Second, even if we had, what would still be necessary is a dynamical theory (certainly involving the motion of the fluids inside and outside of the membrane) in the context of which one could, in principle, prove whether or not the static solution of interest is attained asymptotically from, say, some initial axisymmetric shape and velocity distribution. From this point of view the members of the family 6^- are not observed because they are not accessible from the dynamical states ordinarily encountered by the red cell; however it would be interesting to see what, if anything, would transpire if a cell in the configuration of the swelling sequence corresponding to $p=7.4$ were subjected to mechanical agitation.

As mentioned in the introduction the equilibrium equations of an elastic shell also possess solutions which reproduce the swelling sequence, so this capability is not unique to our model. Zarda (1975) and Zarda et al. (1975) discuss both the formation of the biconcave disc from the spherical nucleated red cell and the swelling of the biconcave disc to a sphere. In their view the biconcave shape is attained in the following way: a newly formed red cell ejects its nucleus, closes and adopts a spherical shape as a natural (stress and couple free) configuration, this sphere buckles, preserving its area, under an excess of external pressure (in this elastic buckling increased deformation of the sphere corresponds to decreased external pressure) until the biconcave shape is attained. Once the cell has adopted this shape, the stresses and the couples somehow relax, the interior and exterior pressures equalize and the biconcave disc becomes the new natural configuration of the shell. The swelling of the cell may then take place as the internal pressure excess is increased from zero. For their estimates of the elasticity and the bending rigidity of the shell and external pressure excess of 17.46 dynes/cm^2 is required to irreversibly buckle the newly formed cell into the biconcave disc shape given by Fung and Tong (1968) and an internal pressure excess of 110.42 dynes/cm^2 is required to reversibly swell the cell without change in area from this biconcave disc to a sphere.

In our view, after ejection of the nucleus, the spherical cell is buckled reversibly into the biconcave disc by an excess of external osmotic pressure; swelling of this biconcave disc into a sphere occurs when the external pressure excess is diminished. In order to obtain an estimate of the external pressure excess $\bar{p}_d$ associated with the biconcave disc geometry we recall that the physical pressure $\bar{p}$ is

given in terms of the nondimensional pressure p, the curvature elasticity c and the radius of the spherical cell ρ through equation (3.9) as

$$\bar{p} = c\,\rho^{-3}\,p. \tag{5.1}$$

Adopting Helferich's (1973) estimate for the curvature elasticity as $c = 10^{-12}$ erg, we take $\rho = 3.35 \times 10^{-4}$ cm and estimate $p = 7.75$ for the biconcave disc. Then $\bar{p}_d = .205$ dynes/cm^2, while the decrease $\Delta\bar{p}$ in excess pressure necessary to swell the biconcave disc ($p = 7.75$) to the sphere ($p = 6.00$) is $\Delta\bar{p} = .046$ dynes/cm^2. We note that if, in modeling the membrane as a thin elastic shell, the buckling of the spherical cell to the biconcave disc we assumed to be reversible, abandoning the idea that the biconcave disc is adopted as the new natural configuration, the explaination of the shape of the red cell and the swelling sequence would be similar in the two theories. The important difference which would remain is that to swell the elastic shell would require an increase in the external pressure excess.

Rand and Burton (1964) have attempted to measure the difference between the internal and external pressure in red cells by drawing the cells into thin pipettes. They were unable to obtain measurements of the changes in the pressure difference during swelling but do report a determination of the pressure difference for both normal and ellipsoidal cells to be 227.4 dynes/cm^2 internal excess. However in their analysis of the experimental data they use Laplace's law of surface tension for the normal force balance which applies neither to elastic shells nor to the liquid cyrystal surface (for which equation (2.35) should be used).

It may be possible to obtain direct confirmation of some of the predictions of the liquid crystal model by careful observations of both normal and swollen red cells. For example, for cells with similar membranes (the same curvature elasticity c) in the same environment (subject to the same physical pressure $\bar{p}$), the cells with the larger surface area (larger ρ) will, according to equation (3.9), be subject to a greater buckling pressure p and, consequently, will be more deformed. This is consistent with the obervations of Canham and Burton (1968) that normal cells with larger volumes (and hence, by their measurements, larger areas) are thinner, or more biconcave. In the same way cells which have suffered a loss of membrane material are likely to be swollen or, in the extreme, spherical; for, by reducing the area, ρ is decreased and p is diminished, possibly below its value at the first bifurcation. Both cases seem to be observed in the experiments of Rand (1964) who pinched off portions of the membrane of a slightly swollen cell obtaining a small globule and a more swollen biconcave disc.

Although the model of the membrane we have used incorporates a local area constraint while it is generally agreed that the loss of hemoglobin, hemolysis, occurs as a result of area changes in the membrane, it might be worthwhile to close by determining what information about hemolysis this model might provide. One possible necessary condition for the onset of hemolysis is that the mean stress in the surface of the membrane, d, be zero, indicating the transition between mean compression and mean tension. Adopting this as a sufficient condition, hemolysis occurs after the cell has swollen to a sphere, but only if the pressure has

been further reduced to zero. Of course as p is reduced from its value at the first bifurcation, solutions on the first branch of the family 6^- are certainly accessible, but they are energetically unfavorable; so we anticipate that the spherical shape is maintained until hemolysis.

Acknowledgement

I am grateful to Mr. P. C. DiGiulio for his expert assitance with the numerical computations, to Dr. H. Ockendon for several important suggestions, to Dr. J. C. Dunn for many valuable discussions and to my colleagues in the Department of Theoretical and Applied Mechanics for their interest, advice and encouragement. This work was supported in part by a grant from the U.S. National Science Foundation.

Appendix

Here we indicate the relationship between the equilibrium equations (2.28) and (2.29) obtained from the principle of virtual work (2.16) and those of the classical theory of thin elastic shells as derived, for example, by Naghdi (1963).

Suppose c is a curve on the surface A and l is the arc length along c measured from some fixed point on it. The curve is given by equations of the form

$$u^\alpha = u^\alpha(l).$$

The unit vector $\underset{\sim}{t}$ tangent to c is

$$\underset{\sim}{t} = \frac{du^\alpha}{dl}\,\underset{\sim}{a}_\alpha \equiv t^\alpha\,\underset{\sim}{a}_\alpha, \tag{A.1}$$

while the unit vector $\underset{\sim}{\nu}$ in the surface A and normal to c is

$$\underset{\sim}{\nu} = \underset{\sim}{t} \times \underset{\sim}{n} \equiv \nu^\alpha\,\underset{\sim}{a}_\alpha. \tag{A,2}$$

The force $\underset{\sim}{T}$ and the couple $\underset{\sim}{C}$ per unit length of c exerted on the element pierced by $-\underset{\sim}{\nu}$ by the element pierced by $\underset{\sim}{\nu}$ are given in terms of the stress resultants $N^{\alpha\beta}$ and Q^α and the couple resultants $M^{\alpha\beta}$ by

$$\underset{\sim}{T} = N^{\alpha\beta}\,\nu_\alpha\,\underset{\sim}{a}_\beta + Q^\alpha\,\nu_\alpha\,\underset{\sim}{n}, \tag{A.3}$$

and

$$\underset{\sim}{C} = \varepsilon_{\beta\mu}\,M^{\alpha\beta}\,\nu_\alpha\,\underset{\sim}{a}^\mu. \tag{A.4}$$

The equations of equilibrium for a shell subject to hydrostatic loading, expressed in terms of the stress and couple resultants, are

$$N^{\beta\alpha}|_\beta - b^\alpha_\beta\,Q^\beta = 0, \tag{A.5}$$

$$Q^\alpha|_\alpha + b_{\alpha\beta}\,N^{\beta\alpha} - \bar{p} = 0, \tag{A.6}$$

$$M^{\beta\alpha}|_\beta - Q^\alpha = 0, \tag{A.7}$$

and

$$\varepsilon_{\alpha\beta}\,(N^{\beta\alpha} - b^\beta_\gamma\,M^{\gamma\alpha}) = 0. \tag{A.8}$$

If Q^α, the transverse shear, is eliminated from (A.5) and (A.6) the equilibrium conditions become

$$N^{\beta\alpha}|_{\beta} - b^{\alpha}_{\beta} M^{\mu\beta}|_{\mu} = 0, \tag{A.9}$$

$$M^{\beta\alpha}|_{\beta\alpha} + b_{\alpha\beta} N^{\beta\alpha} - \bar{p} = 0, \tag{A.10}$$

and equation (A.8).

If we introduce the constitutive relations

$$M^{\alpha\beta} = -c\, h\, a^{\alpha\beta} \tag{A.11}$$

and

$$N^{\alpha\beta} = -\gamma \sqrt{a}\, a^{\alpha\beta} - c\, h\, b^{\alpha\beta}, \tag{A.12}$$

then (A.8) is satisfied identically, while equations (A.9) and (A.10) yield, respectively, equations (2.29) and (2.28).

By (A.7), the transverse shear is given in terms of derivatives of the couple resultants; consequently

$$Q^{\alpha} = c\, h_{,\beta}\, a^{\alpha\beta}. \tag{A.13}$$

When equation (2.33) is used to eliminate the Lagrange multiplier γ from (A.12) the expression for the surface stress resultants N^{α}_{β} is

$$N^{\alpha}_{\beta} = (-\bar{d} + c\, h^2)\, \delta^{\alpha}_{\beta} - c\, h\, b^{\alpha}_{\beta}. \tag{A.14}$$

The physical significance of the constant $\bar{d}$ may be determined from (A.14) by contracting the indices;

$$-\bar{d} = \tfrac{1}{2} N^{\alpha}_{\alpha}. \tag{A.15}$$

Thus $\bar{d}$ is the negative of the mean stress in the surface.

Note added in proof: Recently Helfrich and Deuling (1975) and Deuling and Helfrich (1976 a, 1976 b) have calculated axisymmetric shapes for red blood cells and other bilayer vesicles. They emphasize the importance of the spontaneous curvature, as elaborated upon by Helfrich (1974), in influencing the shape and determining the stability of the equilibrium configurations. Their axisymmetric equilibrium equation is a first integral, which exists in the axisymmetric case, of an equation corresponding to (2.35). With spontaneous curvature, this modification of equation (2.35) may be obtained by the procedure outlined in the Appendix after replacing the mean curvature in equations (A.11) and (A.14) by the difference between the mean and the spontaneous curvatures. Deuling and Helfrich (1976 b) calculate, for example, a negative critical value for the spontaneous curvature below which oblate ellipsoids involve less energy than prolate ellipsoids in the neighborhood of the first bifurcation. However this result doesn't seem to be consistent with the energetics of the numerical solutions, obtained here for zero spontaneous curvature, shown in the neighborhood of the first bifurcation in Fig. 5 b.

References

Adams, K. H.: Mechanical Equilibrium of Biological Membranes. Biophysical J. *12*, 123—130 (1972).

Adams, K. H.: Mechanical Deformibility of Biological Membranes and the Sphering of the Erythrocyte. Biophysical J. *13*, 209—217 (1973 a).

Adams, K. H.: A Theory for the Shape of the Red Blood Cell. Biophysical J. *13*, 1049—1053 (1973 b).

Bellman, R. E., Kabala, R. E.: Quasilinearization and Nonlinear Boundary Value Problems. New York: American Elsevier 1965.

Canham, P. B., Burton, A. C.: Distribution of Size and Shape in Populations of Normal Human Red Cells. Circ. Res. *22*, 405—422 (1968).

Canham, P. B.: The Minimum Energy of Bending as a Possible Explanation of the Biconcave Shape of the Red Blood Cell. J. Theor. Biol. *26,* 61—81 (1970).

Canham, P. B., Parkinson, D. R.: The Area and Voume of Single Human Erythrocytes During Gradual Osmotic Swelling of Hemolysis. Can. J. Physiol. Pharmacol. *48,* 369—376 (1970).

Deuling, H. J., Helfrich, W.: Red Blood Cell Shapes as Explained on the Basis of Curvature Elasticity. Biophysical J. *16,* 861—868 (1976 a).

Deuling, H. J., Helfrich, W.: The Curvature Elasticity of Fluid Membranes: A Catalogue of Vesicle Shapes. J. Phys. *37,* 1335—1345 (1976 b).

Eisenhart, L.: An Introduction to Differential Geometry. Princeton: Princeton University Press 1947.

Fergason, J. L., Brown, G. H.: Liquid Crystals and Living Systems. J. Amer. Oil Chemists Soc. *45,* 120—127 (1968).

Fung, Y. C.: Theoretical Considerations of the Elasticity of Red Cells and Small Blood Vessels. Federation Proc. *25,* 1761—1772 (1966).

Fung, Y. C. B., Tong, P.: Theory of the Sphering of Red Blood Cells. Biophysical J. *8,* 175—198 (1968).

Helfrich, W.: Elastic Properties of Lipid Bilayers: Theory and Possible Experiments. Z. Naturforsch. *28 c,* 693—703 (1973).

Helfrich, W.: Blocked Lipid Exchange in Bilayers and its Possible Influence on the Shape of Vesicles. Z. Naturforsch. *29 c,* 510—515 (1974).

Helfrich, W., Deuling, H. J.: Some Theoretical Shapes of Red Blood Cells. J. Phys. *36-cl,* 327—329 (1975).

Jenkins, J. T.: The Equations of Mechanical Equilibrium of a Model Membrane. S.I.A.M., J. Appl. Math. (to appear).

Lew, H. S.: Effect of Membrane Potential on the Mechanical Equilibrium of Biological Membranes. J. Biomech. *3,* 569—582 (1970).

Lew, H. S.: Electro-tension and Torque in a Biological Membrane Modeled as a Dipole Sheet in Fluid Conductors. J. Biomech. *5,* 399—408 (1972).

Naghdi, P. M.: Foundations of Elastic Shell Theory, in: Progress in Solid Mechanics, Vol. IV (Sneddon, I. N., Hill, R., ed.), pp. 3—90. Amsterdam: North-Holland 1963.

Rand, R. P., Burton, A. C.: Mechanical Properties of the Red Cell Membrane I. Membrane Stiffness and Intracellular Pressure. Biophysical J. *4,* 115—135 (1964).

Rand, R. P.: Mechanical Properties of the Red Cell Membrane II. Viscoelastic Breakdown of the Membrane. Biophysical J. *4,* 303—316 (1964).

Rand, R. P.: Some Biophysical Considerations of the Red Cell Membrane. Federation Proc. *26,* 1780—1784 (1967).

Singer, S. J., Nicolson, G. L.: The Fluid Mosaic Model of the Structure of Cell Membranes. Science *175,* 720—731 (1972).

Skalak, R., Tozeren, A., Zarda, R. P., Chien, S.: Strain Energy Function of the Red Blood Cell Membranes. Biophysical J. *13,* 245—264 (1973).

Zarda, P. R., Chien, S., Skalak, R.: Sphering and Formation of Red Blood Cells, in: 1975 Biomechanics Symposium. AMD Vol. 10 (Skalak, R., Nerem, R. N., ed.), pp. 49—52. New York: American Society of Mechanical Engineers 1975.

Zarda, P. R.: Large Deformations of an Elastic Shell in a Viscous Fluid. Ph. D. Dissertation, Columbia University, New York, 1975.

Dr. J. T. Jenkins
Department of Theoretical and Applied Mechanics
Cornell University
Ithaca, N.Y., U.S.A.